HHS Public Access

Author manuscript

Brain Stimul. Author manuscript; available in PMC 2021 May 10.

Published in final edited form as:

Brain Stimul. 2021 ; 14(2): 391–403. doi:10.1016/j.brs.2021.02.005.

Cortical responses to noninvasive perturbations enable individual brain fingerprinting

Recep A. Ozdemir[a,*], **Ehsan Tadayon**[a], **Pierre Boucher**[a], **Haoqi Sun**[b], **Davide Momi**[a,g], **Wolfgang Ganglberger**[b], **M. Brandon Westover**[b], **Alvaro Pascual-Leone**[c,d,e,1], **Emiliano Santarnecchi**[a,f,1], **Mouhsin M. Shafi**[a,1,**]

[a] Berenson-Allen Center for Noninvasive Brain Stimulation, Division of Interventional Cognitive Neurology, Beth Israel Deaconess Medical Center, Boston, MA, USA

[b] Massachusetts General Hospital, Department of Neurology, Harvard Medical School, Boston, MA, USA

[c] Hinda and Arthur Marcus Institute for Aging Research and Deanne and Sidney Wolk Center for Memory Health, Hebrew Senior Life, Boston, MA, USA

[d] Department of Neurology, Harvard Medical School, Boston, MA, USA

[e] Guttmann Brain Health Institute, Institut Guttmann de Neurorehabilitació, Universitat Autonoma de Barcelona, Badalona, Spain

[f] Department of Medicine, Surgery and Neuroscience, University of Siena, Italy

[g] Department of Neuroscience, Imaging and Clinical Sciences, University of Chieti-Pescara, Chieti, Italy

Abstract

* Corresponding author.: rozdemir@bidmc.harvard.edu (R.A. Ozdemir). ** Corresponding author. Berenson-Allen Center for Non-Invasive Brain Stimulation, Beth Israel Medical Center, Harvard Medical School, Boston, MA, USA., mshafi@bidmc.harvard.edu (M.M. Shafi).

[1]contributed equally.

CRediT author contribution statement

Recep A. Ozdemir: designed the study, Conceptualization, conceptualized the framework, Data curation, collected the data, preprocessed the TMS-EEG data, Formal analysis, Writing - original draft, preprocessed and analyzed TMS-EEG data and wrote the first draft. All authors critically reviewed the manuscript for content and approve the final version for publication. **Ehsan Tadayon:** Formal analysis, performed rs-fMRI analysis to define individual TMS targets. All authors critically reviewed the manuscript for content and approve the final version for publication. **Pierre Boucher:** Data curation, collected the data, preprocessed the TMS-EEG data. All authors critically reviewed the manuscript for content and approve the final version for publication. **Davide Momi:** Data curation, collected the data, All authors critically reviewed the manuscript for content and approve the final version for publication. **Alvaro Pascual-Leone:** designed the study, Writing - review & editing, oversaw study conduction and edited the first draft. All authors critically reviewed the manuscript for content and approve the final version for publication. **Emiliano Santarnecchi:** overviewed the selection of stimulation sites. All authors critically reviewed the manuscript for content and approve the final version for publication. **Mouhsin M. Shafi:** designed the study, Conceptualization, conceptualized the framework. overviewed the selection of stimulation sites, Writing - review & editing, oversaw study conduction and edited the first draft. All authors critically reviewed the manuscript for content and approve the final version for publication.

Declaration of competing interest

The authors declare no competing interests.

Appendix A. Supplementary data

Supplementary data to this article can be found online at https://doi.org/10.1016/j.brs.2021.02.005.

Background: In recent years, it has become increasingly apparent that characterizing individual brain structure, connectivity and dynamics is essential for understanding brain function in health and disease. However, the majority of neuroimaging and brain stimulation research has characterized human brain function by averaging measurements from groups of subjects and providing population-level inferences. External perturbations applied directly to well-defined brain regions can reveal distinctive information about the state, connectivity and dynamics of the human brain at the individual level.

Objectives: In a series of studies, we aimed to characterize individual brain responses to MRI-guided transcranial magnetic stimulation (TMS), and explore the reproducibility of the evoked effects, differences between brain regions, and their individual specificity.

Methods: In the first study, we administered single pulses of TMS to both anatomically (left dorsolateral prefrontal cortex- 'L-DLPFC', left Intra-parietal lobule- 'L-IPL) and functionally (left motor cortex- 'L-M1', right default mode network- 'R-DMN, right dorsal attention network- 'R-DAN') defined cortical nodes in the frontal, motor, and parietal regions across two identical sessions spaced one month apart in 24 healthy volunteers. In the second study, we extended our analyses to two independent data sets (n = 10 in both data sets) having different sham-TMS protocols.

Results: In the first study, we found that perturbation-induced cortical propagation patterns are heterogeneous across individuals but highly reproducible within individuals, specific to the stimulated region, and distinct from spontaneous activity. Most importantly, we demonstrate that by assessing the spatiotemporal characteristics of TMS-induced brain responses originating from different cortical regions, individual subjects can be identified with perfect accuracy. In the second study, we demonstrated that subject specificity of TEPs is generalizable across independent data sets and distinct from non-transcranial neural responses evoked by sham-TMS protocols.

Conclusions: Perturbation-induced brain responses reveal unique "brain fingerprints" that reflect causal connectivity dynamics of the stimulated brain regions, and may serve as reliable biomarkers of individual brain function.

Keywords

Transcranial magnetic stimulation; Electroencephalography; TMS evoked Potentials; Brain fingerprinting

Introduction

Every human brain has a unique structural and functional profile, and thus likely exhibits different patterns and dynamics of brain activity both at rest and when performing a given task. However, the vast majority of human neuroimaging studies to date have characterized human brain function by averaging measurements from groups of subjects and providing population-level inferences [1,2]. Recent studies that seek to characterize brain connectivity and dynamics at the individual level have employed resting-state neuroimaging techniques (e.g. resting-state functional Magnetic Resonance Imaging-'fMRI' or resting-state electroencephalography) in which direct assessments of causality are not possible [3,4]. External perturbations applied directly to well-defined brain regions can yield fundamental

insights into the causal interactions and dynamics of large-scale brain networks at the individual level [5]. Single pulses of TMS provide such non-invasive perturbations safely and with precise experimental control over an array of stimulation parameters (e.g. stimulus location, timing, intensity and duration). Simultaneously recording fast evolving TMS-evoked cortical responses with electroencephalography (TMS-EEG) can probe causal brain connectivity dynamics with a temporal resolution comparable to the timescale of neural events.

Trans-synaptic effects of TMS have long been established. TMS-induced motor evoked potentials (MEPs) recorded from contralateral extremity muscles following stimulation of the motor cortex demonstrate propagation of TMS-induced activations through structural connections [6–8]. Similarly, TMS of non-motor regions evokes a series of electro-cortical potentials (TEPs) that spread from the perturbed node to other discrete nodes of the stimulated network, thereby providing a snapshot of the connectivity profile of the stimulated node across distributed brain regions [9,10]. Over the past decade, TEPs have been used to directly assess a broad range of neurophysiological properties such as cortical excitability, excitation/inhibition balance, effective connectivity, and integrity of the mechanisms of plasticity. However, despite their abundant spatial and temporal neurophysiological content, the majority of studies have characterized TEPs at the group level with traditional event-related-potential (ERP) averaging metrics [11–15]. Such group averaging approaches have greatly contributed to our examination of normal and pathological brain states. However, they also pose limitations for understanding the neurophysiology of spatially distributed brain responses at the individual level. Specifically, one major consideration is the temporal and spatial data loss in amplitude-based metrics extracted by ERP averaging. Analyses of TEPs with ERP methodology mainly focuses on the waveform morphology, either at a single electrode or in a subset of electrodes over a particular scalp region, in which selected electrodes are first averaged at the subject-level and then further averaged across subjects over a time-window of interest to generate grand ERPs at the group-level. These grand averaged ERPs are then used to identify major waveform peaks to extract voltage amplitude or latency as single-time-point metrics of brain responses to a given stimulation [14]. Such a substantial amount of data reduction caused by group level averaging inevitably ignores the rich spatial-temporal content of TEPs and may discard crucial information that can be potentially used to characterize individual subjects. For example, inter-individual differences in TEP topography at a given time point manifest individual variability in the spatial configuration of activated neural sources [16,17], while individual differences in temporal evolution of such source localized TEPs reflect unique propagation patterns across distinct brain regions. Taken together, TEPs provide a causal connectivity profile of stimulated brain regions [18]. However, the lack of detailed spatial-temporal characterization of TEPs at the individual level considerably limits our understanding of individual response dynamics to external perturbations, and thus restricts translational utility of TEPs both in cognitive and clinical neurosciences [19].

A critical first step for translating spatial-temporal specificity of TEPs into the clinical realm is to assess whether individual-specific signatures in TEPs are reliable across measurements, and more importantly, distinct enough to identify an individual from a large group of subjects. Therefore, in a series of studies, we aimed to characterize individual brain

responses to image-guided TMS, and explore the reproducibility of the evoked effects, differences between brain regions, and their individual specificity. In the first study, we focused on the spatial-temporal evolution of brain responses at the individual level and hypothesized that controlled perturbations of distinct brain regions by TMS will reveal distinctive patterns of activation dynamics reflecting unique connectivity characteristics of the stimulated region for each individual, and thus enable cortical fingerprinting (Study-I). In the second study, we first tested whether our main results from Study-I generalize to other independent data sets, and then examined subject specificity of TEPs against non-transcranial neural responses evoked by two different sham-TMS protocols (Study-II).

Participants and methods

Study-I:

Data collected from 24 healthy, right-handed volunteers (16 male; mean age = 29.67 ± 10.60 years, ranging from 18 to 49 years) were analyzed for this study. Experimental protocols and voluntary participation procedures were explained to all participants before they gave their written informed consent to the study that conformed to the Declaration of Helsinki, and had been approved by the Institutional Review Board of the Beth Israel Deaconess Medical Center, Boston, MA. Participants had no self-reported history of psychiatric or neurological diseases.

Study-II:

The first cohort (Test retest cohort-TRT) consists of 10 typically healthy adult control participants (5 M/5F, age = 43 ± 18.51 yrs) from an ongoing TMS-EEG study focusing on reproducibility of repetitive TMS (rTMS) induced neuromodulation at the cortical (EEG) and cortical-spinal (EMG) level. The second cohort (Epilepsy) consists of 10 typically healthy adult control participants (9 M/1F, age = 42.2 ± 18.8 yrs) from a TMS-EEG study of epilepsy.

Data acquisition—A T1-weighted (T1w) anatomical MRI scan was obtained in all participants and used for neuronavigation for each TMS visit. In each visit, TMS-EEG and TMS-EMG data were collected synchronously. Details of MRI scanning, TMS, EEG and EMG systems for both studies are provided in the supplementary methods.

Experimental procedures

Study-I: We administered single pulses of TMS to both anatomically (left dorsolateral prefrontal cortex- ‘L-DLPFC’, left Intra-parietal lobule- ‘L-IPL) and functionally (left motor cortex- ‘L-M1’, right default mode network- ‘R-DMN, right dorsal attention network- ‘R-DAN’) defined cortical nodes in the frontal, motor, and parietal regions (Fig. 1A) across 2 identical sessions spaced one month apart. All participants underwent two separate TMS-EEG visits for the stimulation of the two anatomical targets (L-DLPFC, and L-IPL) in one visit and the two functional targets (R-DAN and R-DMN) in another visit. Identical re-test visits for each session were performed one month later (Fig. 1A). Details of functional and anatomical target selections are explained in supplementary methods. The order of the visits

and stimulation sites within each visit was fully randomized across participants and was kept identical across the retest sessions.

At the beginning of each visit, the motor hotspot was determined over the hand region of left motor cortex (L-M1) for eliciting motor evoked potentials (MEPs) in the right first-dorsal-interosseous (FDI) muscle. The hotspot was defined as the region where single-pulse TMS elicited larger and more consistent MEPs in the FDI muscle, as compared to abductor pollicis brevis (APB) muscle, with the minimum stimulation intensity. Resting motor threshold (RMT) was determined on the FDI hotspot as the minimum stimulation intensity eliciting at least five MEPs (≥50 μV) out of ten pulses in the relaxed FDI using monophasic current waveforms [8,20]. In compliance with the IFCN safety recommendations, participants were asked to wear earplugs during hotspot and RMT trials to protect their hearing, and to minimize external noise [21]. TMS was administered with a thin layer of foam placed under the coil to minimize somatosensory contamination of the TMS-evoked EEG potentials. To minimize auditory evoked potentials related to the TMS coil click, auditory white noise masking was used throughout the TMS stimulation.

Following determination of RMT, a total of 120 single pulses of TMS were delivered to each stimulation target at an intensity of 120% RMT with randomly jittered (3000–5000 ms) inter stimulus intervals using monophasic waveforms.

Study II: For TRT cohort, 150 single pulses of TMS at 120% of resting motor threshold with randomly jittered 3–5 s inter-stimulus-intervals was delivered using biphasic waveforms. For this cohort, active-TMS is applied to L-M1 and functionally defined L-IPL (See supplementary methods for details). Similar to our original cohort in study-I, we used auditory noise masking to minimize auditory evoked potentials related to the TMS coil click. Each participant completed two identical TMS-EEG visits spaced approximately 2 months in average (mean = 64.27 ± 39.67 days). For IPL stimulation data were collected from 7/10 participants (in 3 participants an error in the stimulation parameters prevented collection of usable data) while all participants successfully completed L-M1 stimulation for both visits. In this cohort, we applied a sham protocol that closely resembles the active stimulation conditions in Study-I (Supplementary Fig. 1A). Specifically, sham-TMS was administered on the motor hot spot of the FDI muscle over L-M1. An active/sham TMS coil (Cool-B65 A/P, Mag-Venture A/S, Farum, Denmark) was flipped to the placebo side and stimulation intensity was kept identical to actual TMS, but with induced currents on the opposite vertical direction to targeted gyri. A 3D printed 3 cm spacer was attached to the placebo side (Mag-Venture A/S, Farum, Denmark) of the coil to further ensure the elimination of residual currents on the placebo side of the coil (Supplementary Fig. 1A). White noise masking was presented through earplug-earbuds at the maximum volume comfortable for each participant. Small current pulses between 2 and 4 mA and proportional to the intensity of actual TMS pulse were delivered over the left forehead, over the frontalis muscle, using surface electrodes (Ambu Neuroline 715 12/Pouch) to approximate somatosensory sensations arising from skin mechanoreceptors and scalp muscles during active-TMS condition [22]. The main goal of this sham protocol was to minimize AEPs as much as possible and focus on SSEPs induced by electrical stimulation.

For the epilepsy cohort, 100 single pulses of TMS at 120% of RMT with randomly jittered 3–5 s inter-stimulus-intervals was delivered using biphasic waveforms. TMS is applied to L-M1 and anatomically defined L-IPL, and L-LDLPFC (See supplementary methods for details). Each participant completed two identical TMS-EEG visits spaced approximately 2.5 weeks in average (mean = 17.5 ± 14.23 days). All participants completed L-IPL, L-LDLPFC and L-M1 stimulation for both visits. In this cohort, we performed a basic sham control to specifically focus on the presence of AEPs. Sham-TMS was delivered to L-M1 with the TMS coil tilted 90 from the active side (Supplementary Fig. 1B). No auditory noise masking or electrical stimulation is used. Participants were only asked to wear earplugs during sham and active-TMS trials to protect their hearing. The main goal of this sham was to minimize SSEPs and focus on the specific contributions of AEPs to active TMS responses.

EEG preprocessing and metrics—All details for preprocessing of EEG data are provided in the supplementary methods. Cosine similarity of TEPs within and between subjects across sessions were computed as follows:

Similarity Index (SI): We first generated a TEP matrix for each subject (from averaged responses) with a fixed window size (385 ms) covering EEG responses from 15 to 400 ms following TMS pulses (See Supplementary Fig. 2). Each TEP matrix contains millisecond voltage values from all channels with a 63×385 matrix size. We then used cosine similarity to quantify similarity index (SI) between matrices as follows:

$$SI_{XY} = \frac{\sum_{i,t=1}^{n}(X_{it} * Y_{it})}{\left(\sqrt{\sum_{i,t=1}^{n} X_{it}^2}\right) * \left(\sum_{i,t=1}^{n} Y_{it}^2\right)}$$

Where SI_{XY} is the cosine similarity between TEP matrices x (visit-1) and y (visit-2) for a given stimulation site (i.e L-DLPFC), and n is the number of channels with X_{it} and Y_{it} are the ith vector of all channels at time t for visit-1 and visit-2 respectively. For joint analyses of TEP similarity we also concatenated TEP matrices from multiple sites with all possible combinations of two (n = 10), three (n = 10), four (n = 5) and five (n = 1) sites and computed the similarity matrix for each of the combinations. We normalized combined TEP matrices from each site with the Euclidean norm to account for the magnitude differences in TEPs across sites before concatenating.

We generated a 24×24-similarity matrix to compute similarity matrix metrics, where each entry in the matrix rows is the SI value between a given subject in visit-1 and all other subjects in visit-2. Thus, the diagonal of the matrix corresponds to the SI for within-subject values across identical visits. The following metrics were computed from each similarity matrix:

Within-subject similarity: The mean of the diagonal cells in each similarity matrix shows the average similarity within subjects across visits.

Between-subject similarity: The mean of each row in the matrix, excluding the diagonal cell, represents the average between-subject similarity for each subject. We then computed the mean of individual averages to determine the overall between-subject similarity of the matrix for each stimulation condition.

Accuracy: We first determined the SI rank of diagonal cells in the matrix for each row. An individual is correctly identified if the diagonal cell has the highest similarity value (rank 1) at the given row and that is counted as a "hit". Accuracy is simply the ratio of number of hits to total number of subjects.

Signal-to-Noise Ratio (SNR): We converted the similarity matrix into a z-matrix. For each row in the matrix, we calculated the standard deviation of similarity scores across all subjects. The cosine similarity for each cell in the row is normalized by this standard deviation to obtain a z-score. The z-score for the diagonal cell thus represents a measure of the signal-to-noise ratio for the self-similarity assessment. The overall SNR is simply computed as the mean of the diagonal in the Z-matrix.

In Study II, we also computed cosine similarity at the millisecond level by removing the t from summation function at the above equation. Similarly, we used voltage values across all electrodes at each time point as a feature vector, where each channel value corresponds to a certain vector index. The result was a similarity time series for each comparison and allowed us to examine within-subject similarity across sessions (Visit-1 vs Visit-2) at the highest temporal resolution possible. We note that for the primary calculation of the similarity measures with active TMS, components corresponding to the auditory-evoked potential (AEPs) were removed.

EEG Source Reconstruction: All TMS evoked EEG source reconstruction was performed using Brainstorm [23]. First, digitized EEG channel locations and anatomical landmarks of each subject were extracted from Brainsight™ (nasion 'NAS', left pre-auricular 'LPA', and right pre-auricular 'RPA' points), and registered onto individual MRI scans in brainstorm. Next, the EEG epochs, −500 ms–1000 ms with respect to TMS pulse for each TMS trial were uploaded, and the average epoch time series was generated for each subject. Forward modeling of neuro electric fields was performed using the open MEEG symmetric boundary element method [24], all with default parameter settings [23]. Noise covariance was estimated from individual trials using the pre TMS (−500 to 0) time window as baseline. The inverse modeling of the cortical sources was performed using the minimum norm estimation (MNE) method with dynamic statistical parametric mapping (dSPM) and constraining source dipoles to the cortical surface. The resulting output of EEG source reconstruction was the MNE current density time series for each cortical vertex.

Additionally, we also computed global-mean-field-power (GMFP) and spectral power of resting state EEG (Pre-TMS period) to compare fingerprinting performance of SI with these well establish electro-cortical metrics (see supplementary methods for further details).

Statistical analysis—All statistical analyses were performed using custom scripts utilizing Matlab statistical toolbox (Version 17A, The MathWorks Inc., Natick, MA). We ran

nonparametric Wilcoxon rank sum test to compare within-subject similarity, between-subject similarity, and SNR metrics across stimulation sites and conditions. The minimum significance level was set as ($p < 0.05$) and corrected for multiple comparisons for all statistical analyses.

Cluster-based permutation paired sample *t*-test statistics were performed to compare similarity time series at each time point across TMS conditions. First, we ran paired sample t-tests at each sample to determine significant time points between each comparison separately. We then computed the length of adjacent significant time points and sum of t-scores for significant time points to determine (1) cluster size and (2) cluster magnitude in the main analyses, respectively. Following main analyses, we performed permutation t-tests ($n = 1000$) by randomly shuffling 50% of subjects across compared TMS conditions (i.e., 50% of subjects shifted from sham-TBS to active-TMS or vice versa) and determined cluster size and magnitude of significant adjacent time points at each iteration. Finally, we re-compute "*p*" values of significant clusters in the main analyses by calculating the probability of their size and magnitude in the permutation analyses. A cluster in the main analyses is considered to survive permutation, and thus significant, only if both the size and magnitude of a given cluster is above 95% of all cluster sizes and magnitudes derived from permutation tests.

Results

Study I

Individual TEPs are unique and different from grand averaged TEPs—We first examined the reproducibility of TEPs at the group level. Consistent with prior studies reporting high test-retest reliability of TEPs [[14]], TEP waveforms were highly reproducible across sessions (L-DLPFC visit1 vs visit2: $r = 0.95$, L-M1 visit1 vs visit2: $r = 0.93$, L-IPL visit1 vs visit2: $r = 0.98$, R-DMN visit1 vs visit2: $r = 0.94$, and R-DAN visit1 vs visit2: $r = 0.89$) at the group level (Fig. 1B). However, individual TEPs differed markedly across subjects and were substantially distinct from the group-average TEP (Fig. 1C), clearly demonstrating that averaged TEPs at the group level do not represent individual response characteristics to perturbations. Nonetheless, TEPs for a given subject were highly correlated across repeated sessions, suggesting that brain responses to perturbations were reproducible within the individual (Fig. 1D). Source reconstruction of TEPs from individual subjects confirmed that high topographic similarity between subjects reflects consistent activation of similar brain regions, whereas topographical differences between subjects reflect distinct propagation patterns of evoked brain activity across distributed brain regions (Fig. 2).

Spatial temporal evolution TMS evoked potentials are stable and unique—Here we tested our main hypothesis and examined whether TMS-evoked propagation patterns are stable across sessions and unique between individuals, thereby enabling brain fingerprinting. We also examined whether these properties are a result of the perturbation rather than an invariant feature of the ongoing background EEG activity. Thus, we computed the cosine similarity of 1) rs-EEG before TMS and 2) the spatial-temporal evolution of TEPs for a

single stimulation site (LDLPFC), both within- and between-subjects, across sessions (Fig. 3). The resulting similarity matrix for rs-EEG (Fig. 3A, left-panel) revealed poor fingerprinting performance with only 12.5% identification accuracy and with low SNR values (Fig. 3B). On the other hand, the resulting similarity matrix for TMS-EEG (Fig. 3A, right-panel) demonstrated that TEPs from different visits were substantially more similar within than between individuals. On average, similarity for within-subject TEP topographies (0.61) was significantly higher than between-subject similarity indices (0.24; $p < 0.001$), thereby allowing an individual subject to be identified with 74% accuracy.

Interregional differences in test-retest similarity of TEPs—We examined whether similarity of TEPs changes as a function of the stimulation site (Fig. 4A). Highest accuracy for identifying subjects across repeat sessions was achieved for L-DLPFC, followed by L-M1 and L-IPL stimulation (Fig. 4B), indicating that L-DLPFC stimulation generates more unique spatial-temporal pattern across individuals. Although R-DAN stimulation has the lowest accuracy (47%), it was considerably above the chance level (4.3%). Signal-to-noise ratios (SNR) for L-DLPFC stimulation was significantly higher than R-DMN (LDLPFC vs DMN: $Z_{=}2.88$, $p = 0.003$), while no other comparison was significant after correcting for multiple comparisons ($p > 0.05$). Between-subject similarity was highest in L-M1 stimulation (0.30) and it was significantly different from DMN (M1vs DMN: $Z_{=}3.94$, $p = 0.0007$), suggesting that TMS of M1 produces more generic brain responses across subjects.

Combined TEPs from multiple sites reveals unique cortical neurophysiology —We next combined and jointly analyzed TEPs induced by TMS to multiple sites to characterize individual evoked brain dynamics across different brain regions (Fig. 5A). Signal-to-noise ratio (SNR) gradually increased from a single site (1.90) to five site (4.05) combinations, with significant differences between averages of single-site and two-site ($Z_{=}3.74$, $p = 0.001$), and between two-site and three-site ($Z_{=}3.13$, $p = 0.001$) combinations, primarily due to a decrease in between-subject similarity. Perfect (100%) accuracy in fingerprinting individual subjects was achieved by considering the response to perturbation across five sites (Fig. 5B), suggesting that the patterns of perturbation-evoked dynamics are a defining and unique feature of each individual human brain. This is also consistent with our control analyses showing that TEPs are specific to the stimulated region (Supplementary Fig. 3), and provide a more unique characterization of individual brain dynamics as compared to other widely used electrophysiological metrics such as resting state power spectra or the Global Mean Field activation produced by the TMS pulse (Supplementary Figs. 4 and 5).

Study II

Subject specificity of TEPs is generalizable across independent data sets—Main fingerprinting results from both cohorts were provided in Fig. 6. We first replicated our original findings for active-TMS conditions in both data sets with high fingerprinting accuracies ranging from 80 to 100%. Similar to our original results, L-M1 had highest between-subject similarity among the active-TMS conditions in both data sets with significant differences from L-IPL (L-M1 vs L-IPL: $Z_{=}2.65$, $p = 0.041$) in the TRT data set (Fig. 6A, right middle panel). Accordingly, L-IPL had significantly higher SNR in the TRT

cohort than M1 (L-M1 vs L-IPL: $Z_{=}$ −2.87, p = 0.043). Similarly, L-DLPFC had the highest SNR in the epilepsy cohort with significant differences from L-M1 (L-DLPFC vs L-M1: $Z_{=}$3.21, p = 0.022), suggesting that spatial-temporal characteristic of TEPs originating from non-motor cortices are considerably different between individuals but highly reproducible within the individual across sessions (Fig. 6A and B).

On the other hand, fingerprinting results from sham-TMS are markedly different across data sets and provide interesting insights regarding the spatial-temporal propagation patterns of non-transcranially evoked responses (non-TEPs). For the TRT cohort, sham-TMS (Fig. 6A, left upper panel) produced 50% accuracy (Fig. 6B, right upper panel), comparable between-subject similarity and SNR to L-M1 ($p > 0.05$), but significantly higher between-subject similarity (Sham-TMS vs L-IPL: $Z_{=}$2.87, p = 0.029) and lower SNR (Sham-TMS vs L-IPL: $Z_{=-}$4.21, p = 0.015) than L-IPL (Fig. 2B, right middle and lower panels). For the epilepsy cohort, sham-TMS resulted in 80% accuracy (Fig. 6B, right upper panel). However, sham-TMS had substantially higher between-subject similarity (Fig. 2B, right middle panel) than all active-TMS conditions (Sham-TMS vs L-M1: $Z_{=}$4.68, p = 0.011; Sham-TMS vs L-IPL: $Z_{=}$4.93, p = 0.010; Sham-TMS vs L-DLPFC: $Z_{=}$5.27, p = 0.009). Accordingly, sham-TMS had significantly lower SNR (Fig. 6B, right lower panel) than all the active-TMS conditions (Sham-TMS vs LM1: $Z_{=-}$2.24, p = 0.045; Sham-TMS vs L-IPL: $Z_{=-}$2.98, p = 0.027; Sham-TMS vs L-DLPFC: $Z_{=-}$4.31, p = 0.010). Additionally, between-subject similarity in sham-TMS from epilepsy cohort was also significantly higher than sham-TMS from TRT cohort ($Z_{=}$2.91, p = 0.028).

We further examined the role of AEPs in fingerprinting performance in both sham-TMS data sets and computed cosine similarity across visits (sham-TMS in visit-1 vs sham-TMS in visit-2) at the millisecond resolution with and without keeping AEP components. We first compared within-subject similarity between the two sham-TMS conditions in the different cohorts, and found that sham-TMS from epilepsy cohort has significantly higher within-subject similarity in the 80–120 ms and 180–250 ms time windows, suggesting that presence of stronger AEP components in the epilepsy cohort increases within-subject similarity at time windows consistent with the temporal peaks of AEPs (Fig. 7).

Next, we computed within-subject similarity time series for active-TMS conditions across sessions (See supplementary methods for details). We used these time series as our reference points and compared them with similarity time series obtained by computing cosine similarity between sham-TMS in visit-1 and active-TMS conditions in visit-2. Our goal was to examine the extent to which the spatial-temporal characteristics of sham-evoked non-TEPs are shared by active-TMS evoked TEPs. Thus, we combined data sets from both cohorts and computed the similarity between sham and active-TMS conditions for each site (Fig. 8). As expected, we found high similarity between sham-TMS and active-TMS conditions when AEP components were present in both data sets (Fig. 8A, blue colored time series). As such, the similarity time series for sham-TMS in visit-1 and active-TMS in visit-2 were not significantly different from the similarity time series for active-TMS conditions across visits (Fig. 8A, red colored time series). Accordingly, removing AEP components substantially reduces similarity between sham-TMS and active-TMS across visits, while

within-subject similarity in active-TMS conditions remained high even after removing AEPs (Fig. 8B).

Finally, we examined whether the remaining non-TEPs in shamTMS datasets fingerprint TEPs in active-TMS after removing AEP (as done in our original analysis of active-TMS presented in Figs. 4–5 above). Our analyses showed very poor fingerprinting performance for sham-TMS fingerprinting all active-TMS conditions both in TRT and Epilepsy cohorts (Fig. 9), with accuracies ranging only 20%–40%, and low SNR values, altogether suggesting that individual response specificity in active-TMS is distinct from the residual sham-TMS responses after removing AEPs.

Discussion

The characterization of the individual connectome and resulting connectivity dynamics is critical to understanding brain function in both health and disease. Here, we used single pulse TMS to perturb different cortical nodes in frontal, motor, and parietal regions in both hemispheres, and evaluated the resulting evoked spatiotemporal patterns of brain activation at the individual level using EEG. In the first study, in a primary cohort of 24 subjects, we find that such direct, controlled external perturbations of discrete cortical regions generate a sequence of individually distinct yet highly reproducible brain responses, revealing a unique “fingerprint” of dynamical connectivity. In the second study, we confirmed our original findings in two independent data sets each with different sham-TMS controls, suggesting that subject specificity of brain responses to perturbations of discrete brain regions is robust across data sets, and is due primarily to the transcranial-evoked stimulation rather than non-transcranial sensory features. Overall, these results thus illustrate that the patterns of perturbation-evoked dynamics are defining features of each individual human brain, and that TMS-EEG provides a reliable means of characterizing these individual-specific causal propagation patterns.

Grand averaging ignores individual information in TMS evoked potentials

Recent studies examining the reliability of TMS-EEG responses reported that amplitude-based TEP metrics at mid-latencies are reproducible at the group level, but highly variable across subjects [14,25]. Our initial TEP analyses confirmed these prior findings that averaging TEPs across subjects generates reproducible waveforms across sessions at the group level. However, we find that this group-level response poorly overlaps with individual response dynamics, and thus does not represent the actual TMS-induced activation profile for most individuals. Importantly, however, we also find that while brain responses to TMS are markedly different across individuals and distinct from the group mean. This similarity in TEPs across sessions within individuals reflects consistent activation of distributed brain regions over time, whereas differences in TEPs across subjects reflect distinct sequences of brain activity.

We specifically focused on capturing propagation dynamics of TMS-induced activations at the individual level, without employing any data reduction approach either in the spatial (i.e., averaging electrodes) or temporal (i.e., selecting only waveform peaks) domain. Our results demonstrate that characterizing the whole-brain spatial-temporal response dynamics

provoked by TMS generates individually distinct information about the causal connectivity dynamics of the stimulated networks, and that this information is otherwise not observable through traditional group-level averaging metrics and resting-state EEG recordings. Notably, the spatial-temporal response patterns at the individual level are also specific to the stimulated brain regions and highly reproducible between sessions. Combining such site-specific information across multiple brain regions reveals an individually unique brain "fingerprint", capable of identifying each participant with perfect accuracy. Additionally, we also showed that fingerprinting sensitivity and specificity of TMS perturbations substantially outperformed widely used electrophysiological metrics, suggesting that cortical fingerprinting is a specific function of individual differences in spatial propagation characteristics of TEPs.

Utility of perturbation responses in characterizing individual connectivity

Given the high translational and clinical potential of establishing brain-behavior relationships at the individual level, recent neuroimaging studies have focused on characterizing inter-individual variability in brain connectivity with the goal of identifying biomarkers of individual brain function. So far, blood-oxygenation level-dependent (BOLD) functional magnetic resonance imaging (fMRI) during "unconstrained resting" has been the primary neuroimaging tool for characterizing the individual variation in functional brain organization. However, the slow time-course of the hemodynamic response function underlying the BOLD signal, as well as the purely correlational nature of resting-state fMRI connectivity, are two fundamental limitations of this approach for capturing causal brain interactions at the timescale of neuronal activity. In contrast, controlled perturbations (e.g. via TMS) applied directly to well-defined brain regions, including specifically association cortices that underlie higher-order control functions and that show the greatest variability between individuals [7], can yield fundamental insights into the causal interactions and dynamics of large-scale brain networks at the individual level. In particular, TMS of cortical nodes in parietal association cortex has been shown to induce network specific propagation patterns [5] compatible with the functional connectivity profile of the stimulated nodes, endorsing targeted network perturbation as a promising approach to evaluate the causal interactions and dynamics of large-scale brain networks at the individual level. As such, TMS-based assessments of individual connectivity dynamics can complement and extend more traditional resting-state or task-based measures. As an example, a large body of recent human fMRI studies have reported extensive between-subject variance in functional and structural connectivity profile at multimodal association cortices (i.e., frontoparietal or ventral attention) as compared to unimodal sensori-motor cortices [26–28]. Consistent with this, we showed that TMS of motor cortex generated more similar TEP topographies across subjects in three independent data sets, confirming common response dynamics across subjects, as compared to TMS of association cortex sites.

TMS fingerprinting versus non-transcranial evoked activity

A potential confound in TMS-EEG responses could be the contamination of TEPs with non-transcranial sensory-evoked responses such as the auditory evoked potentials (AEP). In our primary analysis cohort, we used noise masking to try to minimize the presence of the AEP component, and used an ICA-based approach in postprocessing to remove residual AEP

elements. However, to determine the potential influence of the AEP on the similarity measures assessed here, we analyzed two additional control datasets, one with noise masking and one without, and including two different types of sham stimulation. We noticed strong AEPs in all subjects in the control epilepsy cohort in which noise masking was not done, while AEPs were observed in only 3 out of 10 subjects in the control test-retest cohort with noise masking, corroborating with the recent evidence [29] that the use of noise masking (as done in our primary study cohort) effectively eliminates or removes AEPs for most of the subjects. Our analyses of sham-TMS data sets showed that, when present, AEPs dominate sham-TMS responses and result in high degree of within-subject similarity across visits. These results suggest that evoked responses in the brain, even when they are non-transcranial (i.e. AEP), may be stable over time. Given the fact that all these sensory evoked responses are processed in individual brains with stable structural connectivity profiles, it is not surprising to observe high within-subject similarity in sensory responses evoked by sham-TMS across sessions. However, the spatial-temporal characteristics of these AEPs are also highly common across subjects, as the uniqueness of each subject's cortical response profile is substantially lower than response characteristics originating from active-TMS of associative cortices. We also found that both within-subject and between-subject similarity are significantly decreased in sham-TMS data sets after AEPs are removed in postprocessing, further confirming that the nature of high within-subject similarity, especially in the epilepsy cohort, heavily depend on the presence of AEPs. In contrast, active-TMS evoked potentials provide excellent fingerprinting with high similarity within each individual and highly distinct propagation patterns across individuals after removing the AEP component. Importantly, when AEPs are removed from both active- and shamTMS data sets, the remaining sham-TMS responses did not effectively fingerprint active-TMS responses, indicating that individual response specificity in active-TMS is unlikely to be due to the presence of residual non-TEPs in active-TMS.

Somatosensory-evoked potentials (SSEPs) could represent another transcranial-evoked component that contributes to the observed effects. Specifically, high between-subject similarity derived from the motor cortex stimulation could be attributed in part to sensory afference evoked by the stimulated muscle. Indeed, in both our test-retest and epilepsy cohorts, sham-TMS responses had the highest similarity with active-TMS responses from L-M1, and the sham-M1 similarity remained significantly higher than the similarity between sham-TMS and active-TMS responses from non-motor cortices after removing AEPs. Moreover, between-subject similarity with M1 stimulation was comparable to sham-TMS between-subject similarity in the test-retest cohort in which we applied electrical stimulation to induce somatosensory sensations. Taken together, these findings suggest that the presence of SSEPs may contribute to the high between-subject similarity seen with M1 stimulation. However, accuracy and SNR were higher with M1 stimulation than with sham stimulation even in the test-retest cohort, suggesting that the observed subject specificity is not just due to the presence of SSEPs. Notably, the between-subject similarity values were significantly lower, and the SNR significantly higher, with stimulation of non-motor associative regions in comparison to sham, suggesting that this somatosensory-evoked component does not play a major role in the fingerprinting accuracy of the unique and reliable evoked potentials obtain from non-motor regions.

Limitations

Certain limitations of the study should be acknowledged. Our subjects from all data sets are young and healthy participants with no known neurological, psychiatric or cognitive disorders. It is therefore essential to evaluate the validity of our results in different age groups (e.g. children, older adults) and in various clinical populations, to establish the spatial-temporal specificity of TEPs as biomarkers of individual brain function in both health and disease. Another important translational step would be focusing on “between-subject” similarity characteristics to examine whether individuals with similar cortical response signatures at the network level also share common cognitive or behavioral characteristics. Moreover, the stability of cortical response dynamics across multiple repeat sessions with long time intervals is yet to be determined.

Conclusions

TMS-EEG can be used to characterize the causal propagation patterns of brain responses toTMS perturbations at the timescale of normal physiological function. While such TMS-evoked responses are highly reproducible at the group level, individual responses are distinct from the group response and highly heterogeneous across subjects. Nevertheless, the spatiotemporal patterns of individual TMS-evoked responses are stable over time and specific to the stimulated region, carrying information about individual connectivity dynamics that is distinct from spontaneous activity. Most importantly, we demonstrate that an individually unique brain fingerprint can be identified by combining spatial-temporal characteristics of TMS induced brain responses originating from different cortical regions. These results thus reveal spatial-temporal analyses of whole brain responses to neuroimaging-based perturbation as a highly promising approach to characterize causal brain-connectivity dynamics at the individual level. Such perturbation-based characterization of brain responses may serve as reliable biomarkers of individual brain function that could enable the longitudinal tracking of individual brain dynamics across the lifespan, in pathological processes, and in response to therapeutic interventions.

Supplementary Material

Refer to Web version on PubMed Central for supplementary material.

Acknowledgments

We thank all participants who took part in the study for their effort. The study was supported by the Harvard-MIT BROAD Institute (Grant ID 6600024–5500000895). A.P.-L. is supported by the Berenson-Allen Foundation, the Sidney R. Baer Jr. Foundation, NIH Grants R01HD069776, R01NS073601, R21 MH099196, R21 NS082870, R21 NS085491, and R21 HD07616, and The Harvard Clinical and Translational Science Center (National Center for Research Resources and the National Center for Advancing Translational Sciences Grant UL1 RR025758). E.S. is supported by the Beth Israel Deaconess Medical Center via the Chief Academic Officer Award 2017, the Defence Advanced Research Projects Agency via HR001117S0030, and NIH Grants P01 AG031720–06A1, R01 MH117063–01, and R01 AG060981–01. M.M.S. is supported by the Citizens United for Research in Epilepsy foundation, the Football Players Health Study at Harvard University, and NIH Grants R01 MH115949, R01AG060987, R01 NS073601, and P01 AG031720–06A1. The content of this paper is solely the responsibility of the authors and does not necessarily represent the official views of Harvard University and its affiliated academic health care centers, or NIH.

References

[1]. Van Essen DC, et al. The Wu-minn human connectome project: an overview. Neuroimage 2013;80:62–79. [PubMed: 23684880]

[2]. Greicius MD, Krasnow B, Reiss AL, Menon V. Functional connectivity in the resting brain: a network analysis of the default mode hypothesis. Proc Natl Acad Sci Unit States Am 2003;100:253–8.

[3]. Finn ES, et al. Functional connectome fingerprinting: identifying individuals using patterns of brain connectivity. Nat Neurosci 2015;18:1664–71. [PubMed: 26457551]

[4]. Tavor I, et al. Task-free MRI predicts individual differences in brain activity during task performance. Science 2016;352:216–20. [PubMed: 27124457]

[5]. Ozdemir RA, et al. Individualized perturbation of the human connectome reveals reproducible biomarkers of network dynamics relevant to cognition. Proc Natl Acad Sci Unit States Am 2020. 10.1073/pnas.1911240117.

[6]. Hallett M Transcranial magnetic stimulation and the human brain. Nature 2000;406:147–50. [PubMed: 10910346]

[7]. Kobayashi M, Pascual-Leone A. Transcranial magnetic stimulation in neurology. Lancet Neurol 2003;2:145–56. [PubMed: 12849236]

[8]. Rothwell JC, et al. Magnetic stimulation: motor evoked potentials. Electroencephalogr Clin Neurophysiol Suppl 1999;52:97–103. [PubMed: 10590980]

[9]. Ilmoniemi RJ, et al. Neuronal responses to magnetic stimulation reveal cortical reactivity and connectivity. Neuroreport 1997;8:3537–40. [PubMed: 9427322]

[10]. Komssi S, et al. Ipsi-and contralateral EEG reactions to transcranial magnetic stimulation. Clin Neurophysiol 2002;113:175–84. [PubMed: 11856623]

[11]. Bagattini C, et al. Predicting Alzheimer's disease severity by means of TMS–EEG coregistration. Neurobiol Aging 2019;80:38–45. [PubMed: 31077959]

[12]. Bortoletto M, Veniero D, Thut G, Miniussi C. The contribution of TMS–EEG coregistration in the exploration of the human cortical connectome. Neurosci Biobehav Rev 2015;49:114–24. [PubMed: 25541459]

[13]. Darmani G, Ziemann U. Pharmacophysiology of TMS-evoked EEG potentials: a mini-review. Brain Stimulation 2019;12:829–31. [PubMed: 30837122]

[14]. Kerwin LJ, Keller CJ, Wu W, Narayan M, Etkin A. Test-retest reliability of transcranial magnetic stimulation EEG evoked potentials. Brain Stimulation 2018;11:536–44. [PubMed: 29342443]

[15]. Lioumis P, Kičić D, Savolainen P, Mäkelä JP, Kähkönen S. Reproducibility of TMS—evoked EEG responses. Hum Brain Mapp 2009;30:1387–96. [PubMed: 18537115]

[16]. Murray MM, Brunet D, Michel CM. Topographic ERP analyses: a step-by-step tutorial review. Brain Topogr 2008;20:249–64. [PubMed: 18347966]

[17]. Michel CM, Murray MM. Towards the utilization of EEG as a brain imaging tool. Neuroimage 2012;61:371–85. [PubMed: 22227136]

[18]. Hallett M, et al. Contribution of transcranial magnetic stimulation to assessment of brain connectivity and networks. Clin Neurophysiol 2017;128: 2125–39. [PubMed: 28938143]

[19]. Fox MD, et al. Resting-state networks link invasive and noninvasive brain stimulation across diverse psychiatric and neurological diseases. Proc Natl Acad Sci Unit States Am 2014;111:E4367–75.

[20]. Rossini PM, et al. Non-invasive electrical and magnetic stimulation of the brain, spinal cord, roots and peripheral nerves: basic principles and procedures for routine clinical and research application. An updated report from an IFCN Committee. Clin Neurophysiol 2015;126:1071–107. [PubMed: 25797650]

[21]. Rossi S, Hallett M, Rossini PM, Pascual-Leone A. Safety, ethical considerations, and application guidelines for the use of transcranial magnetic stimulation in clinical practice and research. Clin Neurophysiol 2009;120:2008–39. Group, S. of T. C. [PubMed: 19833552]

[22]. Rossi S, et al. A real electro-magnetic placebo (REMP) device for sham transcranial magnetic stimulation (TMS). Clin Neurophysiol 2007;118: 709–16. [PubMed: 17188568]

[23]. Tadel F, Baillet S, Mosher JC, Pantazis D, Leahy, Brainstorm RM. A user-friendly application for MEG/EEG analysis. Comput Intell Neurosci 2011;2011:1–13. [PubMed: 21837235]

[24]. Gramfort A, et al. MNE software for processing MEG and EEG data. Neuroimage 2014;86:446–60. [PubMed: 24161808]

[25]. Rogasch N, et al. TMS-evoked EEG potentials from prefrontal and parietal cortex: reliability, site specificity, and effects of NMDA receptor blockade. bioRxiv 2019. 10.1101/480111.

[26]. Bürgel U, et al. White matter fiber tracts of the human brain: three-dimensional mapping at microscopic resolution, topography and inter-subject variability. Neuroimage 2006;29:1092–105. [PubMed: 16236527]

[27]. Frost MA, Goebel R. Measuring structural–functional correspondence: spatial variability of specialised brain regions after macro-anatomical alignment. Neuroimage 2012;59:1369–81. [PubMed: 21875671]

[28]. Mueller S, et al. Individual variability in functional connectivity architecture of the human brain. Neuron 2013;77:586–95. [PubMed: 23395382]

[29]. Rocchi L, et al. Disentangling EEG responses to TMS due to cortical and peripheral activations. Brain Stimulation 2020;14(1):4–18. 10.1016/j.brs.2020.10.011. ISSN 1935–861X. [PubMed: 33127580]

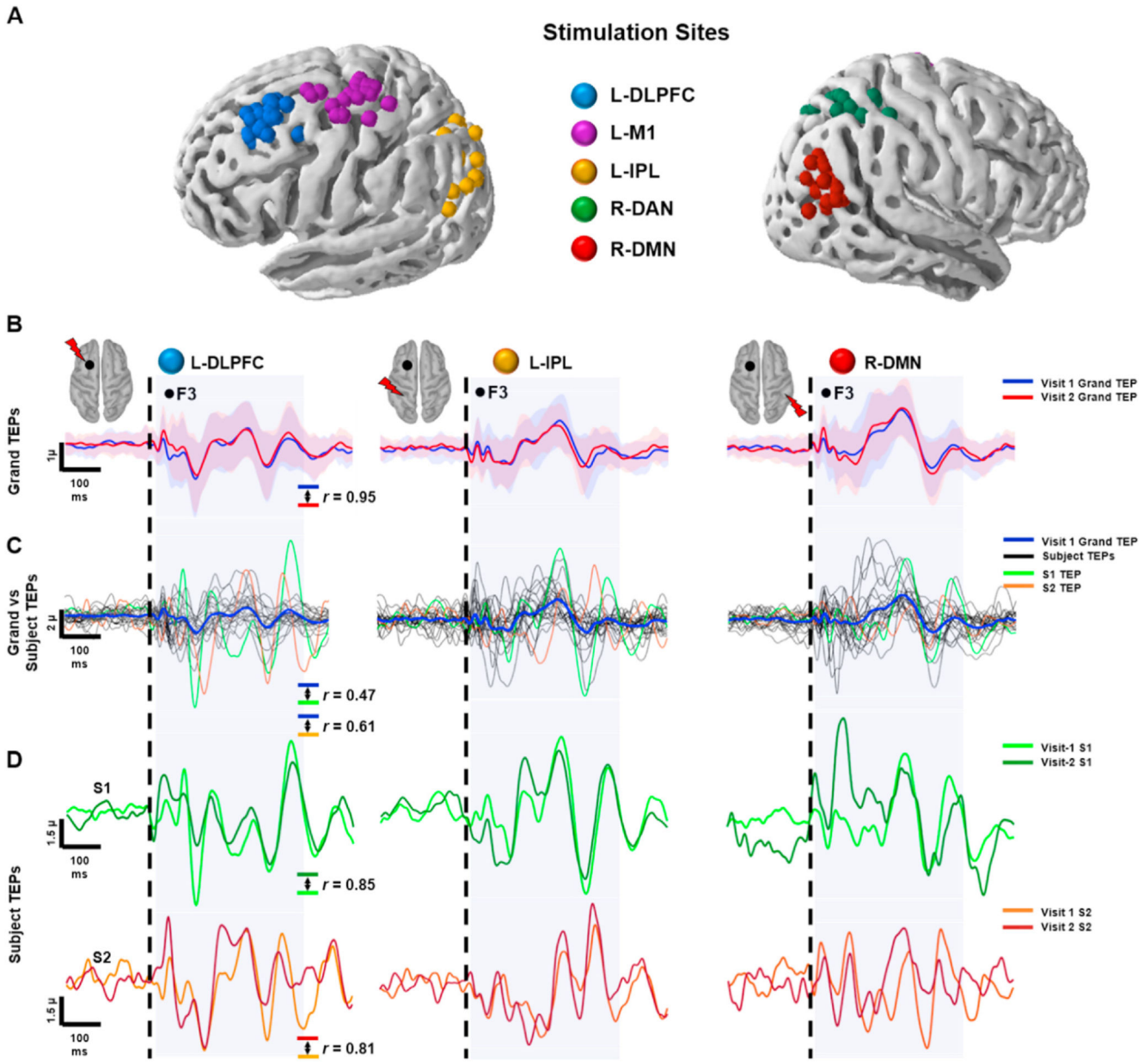

Fig. 1.

Group averaged vs individual TEPs. A: Representation of individual stimulation sites for each cortical region on a template brain. B: Grand averaged TEPs (across all subjects) at the F3 electrode (black dot over the template brains) across visits in response to L-DLPFC (left), R-DMN (middle), and L-IPL (right) stimulations (shades showing variability as one unit of standard deviation). Dotted vertical black lines show TMS. Gray shaded rectangular shows the time range used (15 ms–300 ms) to compute spearman correlation coefficients (r) between the two time series in each panel. C: Individual TEPs (thin colored lines) superimposed over the grand average TEP (thick blue line) in visit-1. D: Representative TEPs from two different subjects across visits.

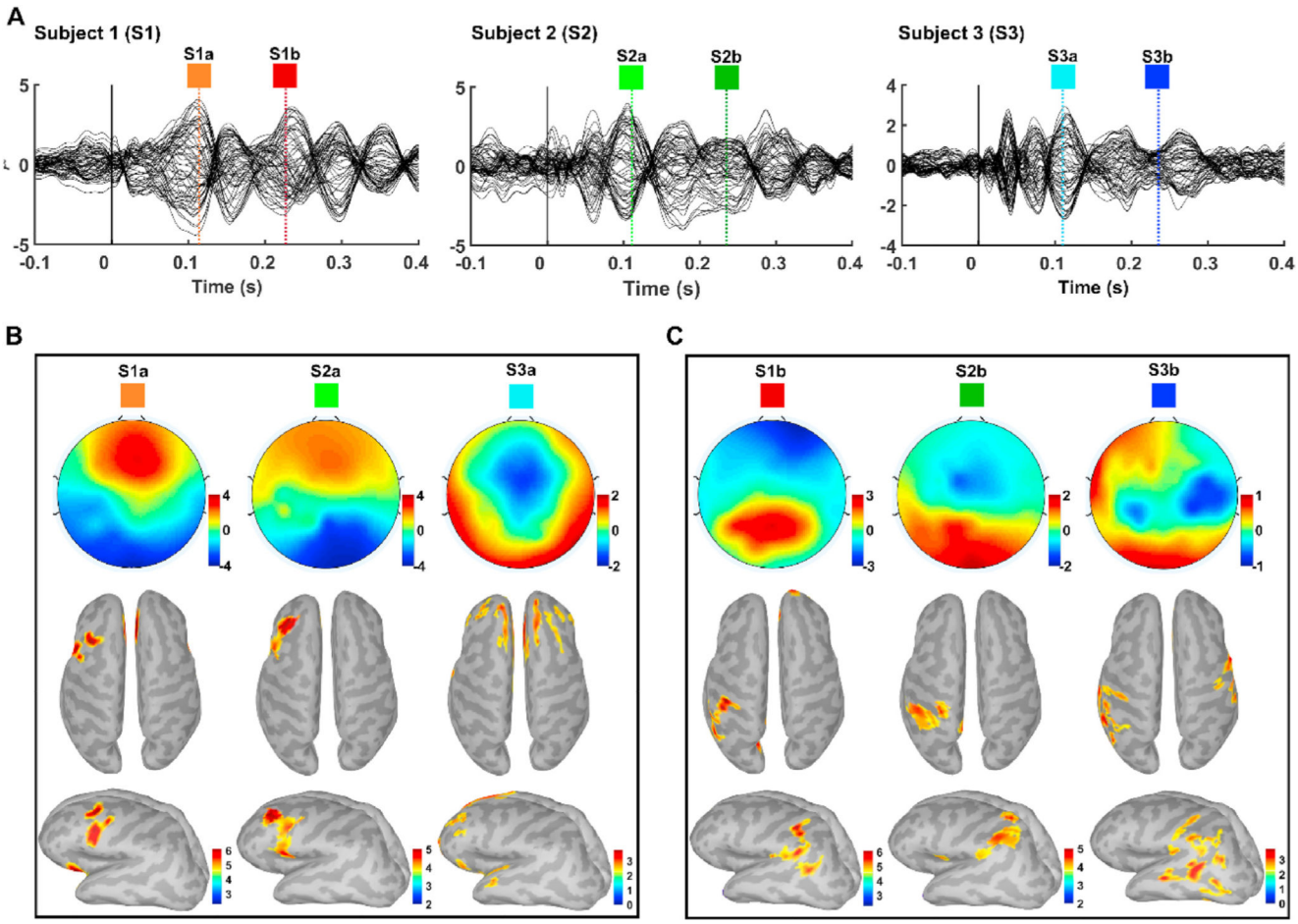

Fig. 2. Source reconstruction of TEPs across subjects with high and low similarity.

A: TEPs from LDLPFC stimulation for three representative subjects (S1, S2 and S3) with selected peaks (colored vertical lines). B and C: topography and corresponding source reconstructions of selected time points in A. Note that subject S1 has a similar topography compared to S2, but different topography from S3; the corresponding source reconstructions of these topographies reflect similar localization of cortical sources and propagation patterns for S1 and S2 but not for S3. (see Supplementary Methods for details of source reconstruction).

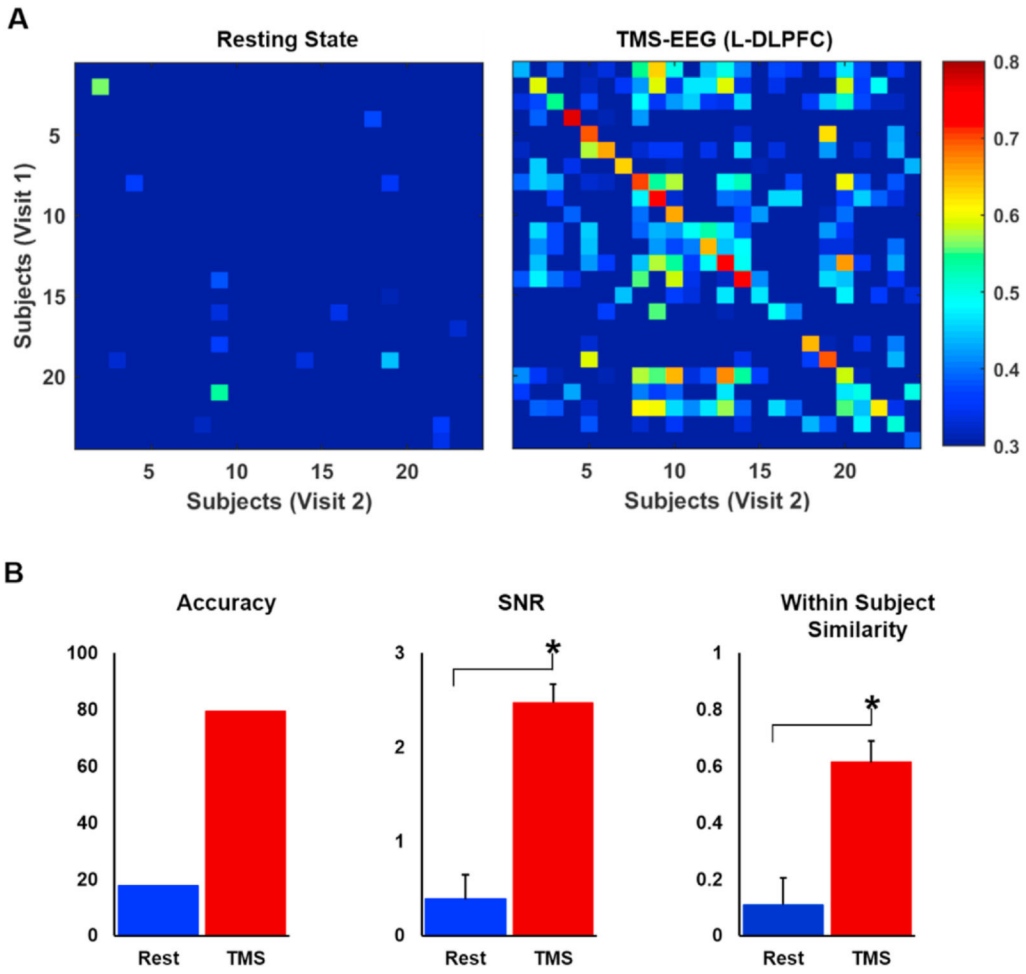

Fig. 3.

Fingerprinting with rs-EEG vs TEPs: A: Similarity matrix for Resting EEG (left) and L-DLPFC stimulation (right). Each color-coded cell represent the magnitude of cosine similarity across repeat sessions. Diagonal cells show each subjects' own cosine similarity while cells in each row (excluding the diagonal) show each subject's cosine similarity with every other subject in the group across repeat sessions. B: Accuracy (left), SNR (middle), and average within-subject similarity (left) metrics computed from the matrices in A. Error bars in B denote one unit of standard error of measurement (SEM), and stars denote significant comparisons across conditions after controlling for multiple corrections.

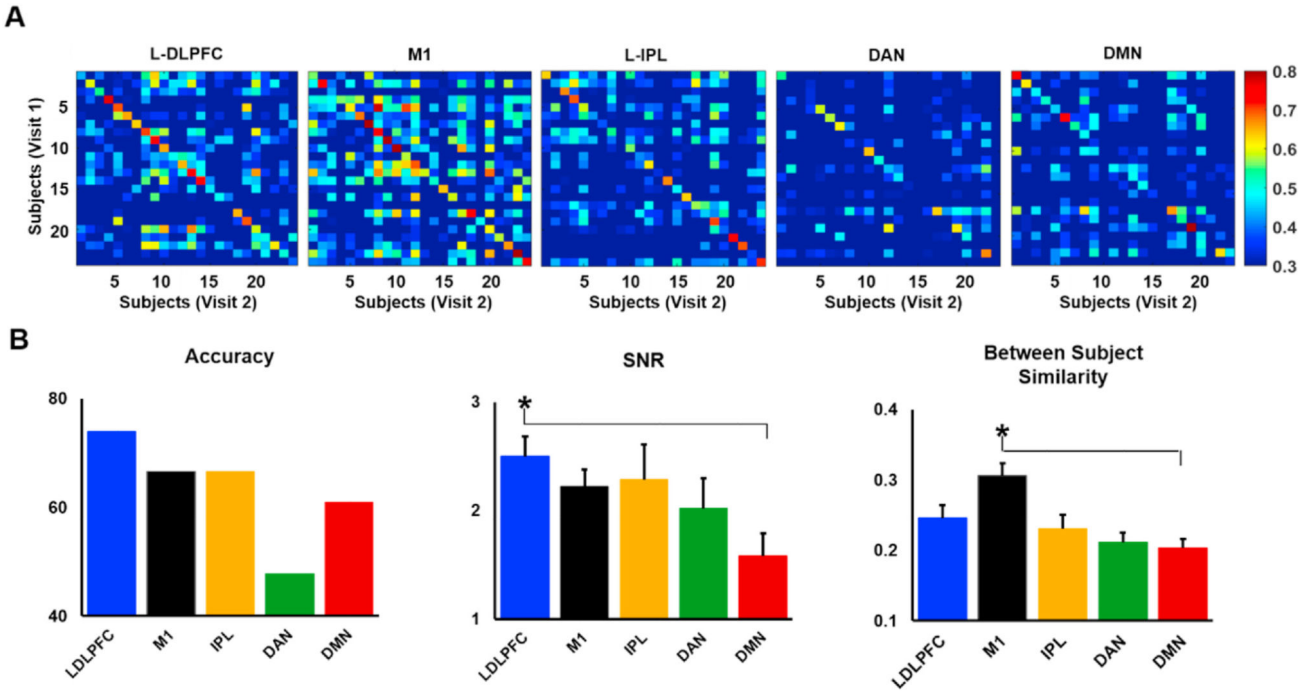

Fig. 4.

Similarity differences across stimulation sites. A: Similarity matrix for each stimulation site across repeat sessions. B: Comparison of similarity matrix metrics. Error bars in B denotes one unit of standard error of measurement SEM, and stars denotes significant comparisons across conditions after controlling for multiple corrections.

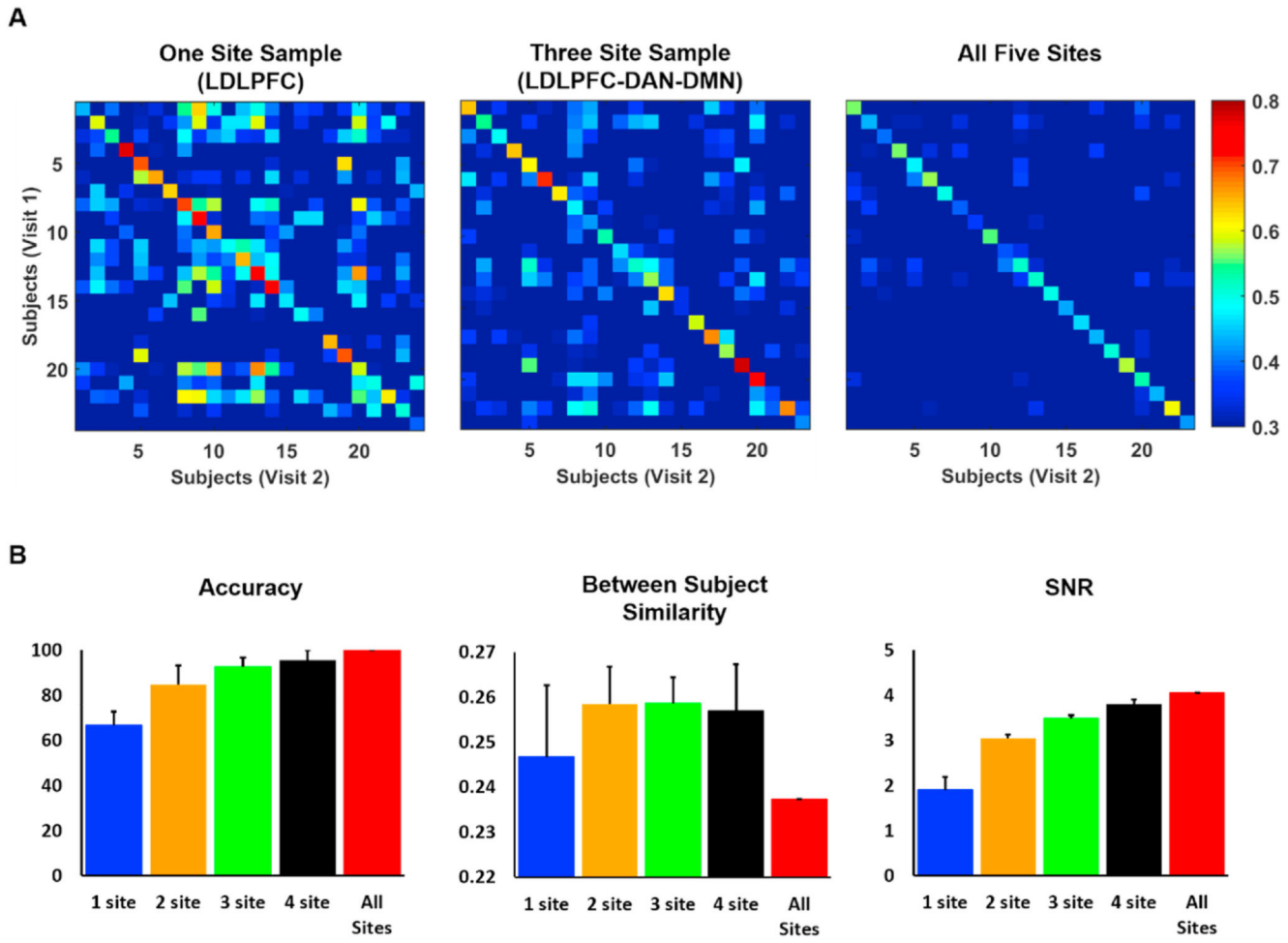

Fig. 5.

Combining TEPs from multiple sites. A: Representative similarity matrices were shown for single site (LDLPFC: left upper panel), combination of three different sites (LDLPFC-DAN-DMN), and combination of five sites. B: Comparison of similarity matrix metrics between single-site, two-site, three-site, four-site and five-site combinations. Bars represent average metric values for all the possible combinations. Error bars represent one unit of SEM.

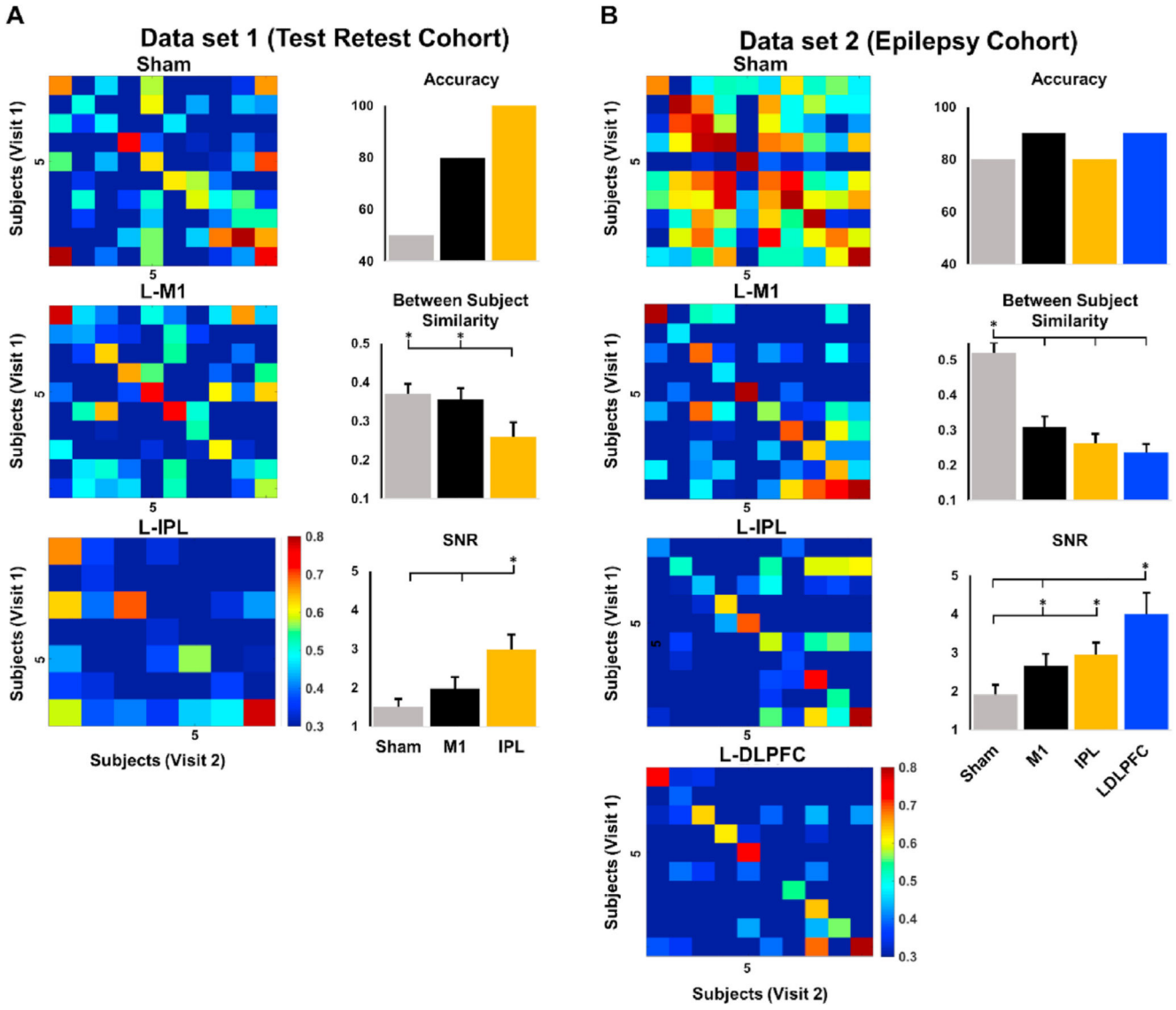

Fig. 6.

Fingerprinting with active- and sham-TMS. A: Results for test retest cohort. Similarity matrices (left panels) and fingerprinting metrics (right panel) for sham-TMS and active-TMS from L-M1 and L-IPL, B: Results for epilepsy cohort. Similarity matrices (left panels) and fingerprinting metrics (right panel) for sham-TMS and active-TMS from L-M1, L-IPL, L-LDLPFC. Error bars in metric panels denotes one unit of standard error of measurement SEM, and stars denotes significant comparisons across conditions after controlling for multiple corrections.

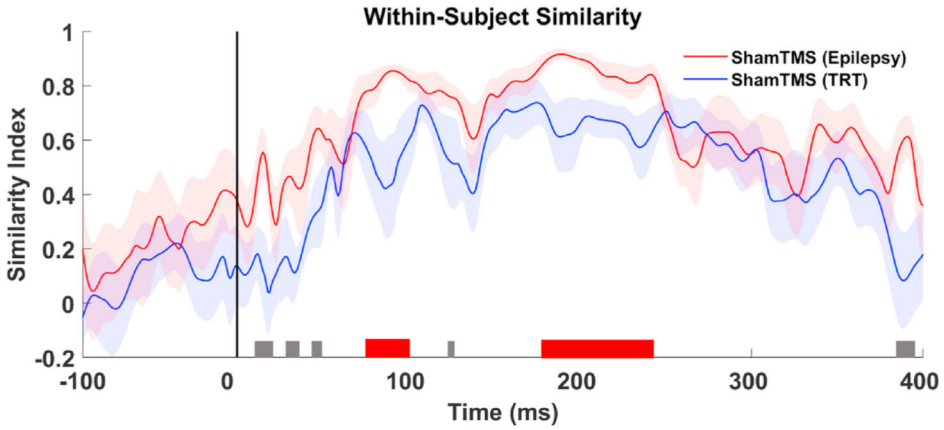

Fig. 7.

Similarity time series of Sham-TMS across visits for each Cohort. Colored lines (Red: Epilepsy cohort, Blue: Test retest “TRT” cohort) represent group averaged within-subject similarity time series across sessions (Visit-1 vs Visit-2) for each cohort, and shaded colored regions represent one unit of standard error of measurement (SEM). Colored blocks at the bottom of each panel show significant cluster of time-points between comparisons (Gray blocks: Significant clusters for bivariate comparisons that did not survive permutation tests and Red Blocks: Significant clusters survived permutation tests $p < 0.05$).).

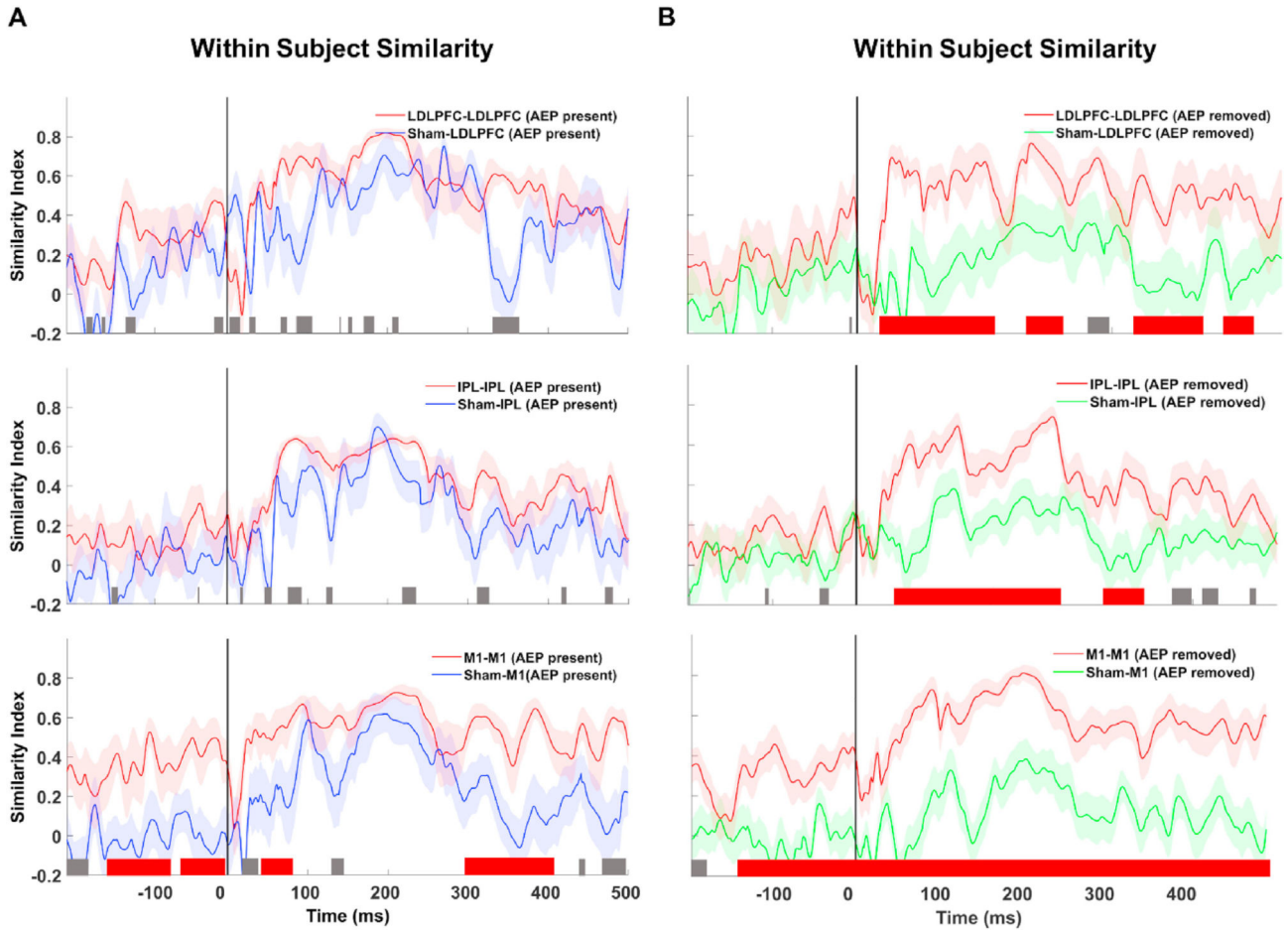

Fig. 8.

Comparison of similarity time series for active-TMS to active-TMS with sham-TMS to active-TMS across visits. A: Comparison of active-TMS to active-TMS with AEPs (red) to sham-TMS to active-TMS (blue) with AEPs. B: Comparison of active-TMS to active-TMS without AEPs (red) to sham-TMS to active-TMS (green) without AEPs. Colored blocks at the bottom of each panel show significant cluster of time-points between comparisons (Gray blocks: Significant clusters for bivariate comparisons that did not survive permutation tests and Red Blocks: Significant clusters survived permutation tests $p < 0.05$).

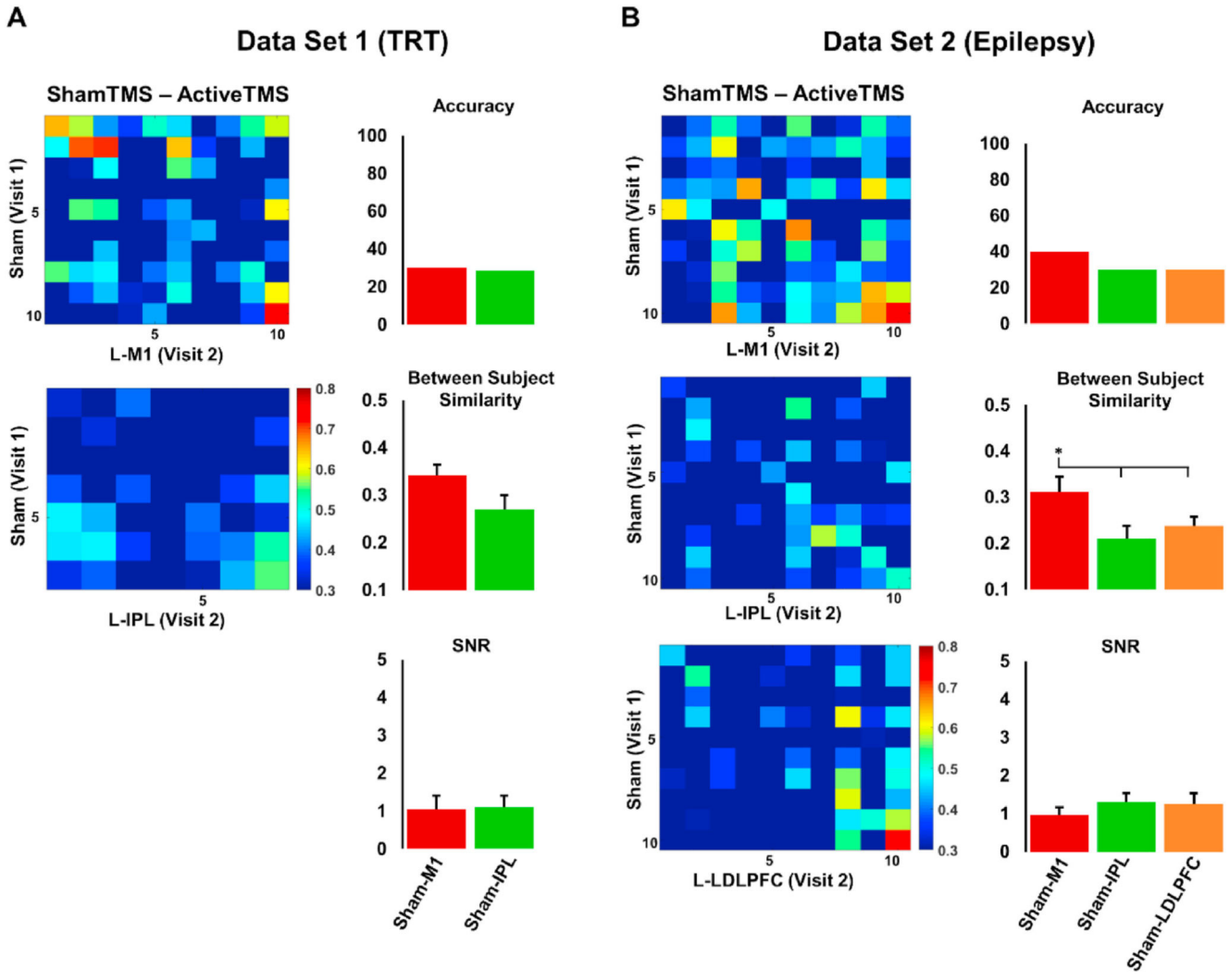

Fig. 9. Fingerprinting active-TMS responses with sham-TMS.

A: Test retest cohort similarity matrices (left panels) and metrics (right panels) for sham-TMS in visit-1 fingerprinting active-TMS from L-M1 (Left upper panel) and L-IPL (Left lower panel) in visit-2. B: Epilepsy cohort similarity matrices (left panels) and metrics (right panels) for sham-TMS in visit-1 fingerprinting active-TMS from L-M1 (Left upper panel), L-IPL (Left middle panel) and L-DLPFC (Left lower panel) in visit-2. Error bars in metric panels denotes one unit of standard error of measurement SEM, and stars denotes significant comparisons across conditions after controlling for multiple corrections.